Clustering Approach for the Efficient Solution of Multiscale Stochastic Programming Problems: Application to Energy Hub Design and Operation under Uncertainty

Mohammed Alkatheri[a], Falah Alhameli[a], Ali Elkamel[a,*], Alberto Betancourt-Torcat[a], Ali Almansoori[b]

[a]Department of Chemical Engineering, University of Waterloo, 200 University Ave. West, Waterloo, ON, Canada N2L 3G1

[b]Department of Chemical Engineering, Khalifa University of Science and Technology, Sas Al Nakhl Campus, Abu Dhabi, P.O. Box 2533, United Arab Emirates

[*]Corresponding author: Tel: +1 519-888-4567 ext. 37157; e-mail: aelkamel@uwaterloo.ca

This Supplementary Material provides additional information on the present study.

1. Clustering Verification

This section aims to assess the computational performance of the proposed general clustering algorithm (full-scale model) and the heuristic algorithm. For instance, a case study of an energy hub system's hourly heat and electricity demands during a year is used for illustration and evaluation purposes (Maroufmashat et al., 2015). Figures S1 and S2 show the heat and electricity demands, respectively .

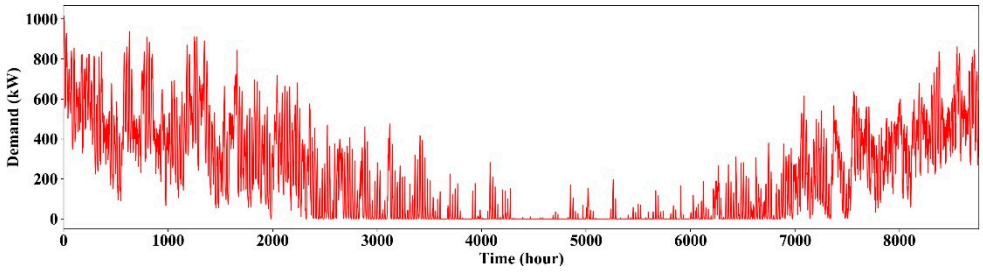

Figure S1. Annual hourly heat demand (Maroufmashat et al., 2015).

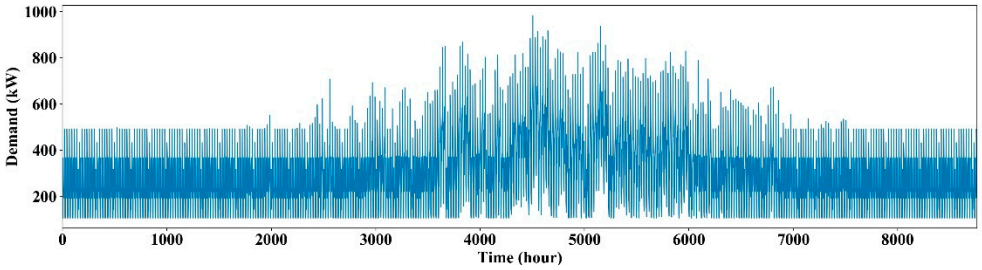

Figure S2. Annual hourly electricity demand (Maroufmashat et al., 2015).

Raw time-series data such as electricity and heat demand are arranged into the candidate periods (considered to be 365 days for 1 year, each day consisting of 24 hours). This reordering process is shown in the matrix shown in Figure S3. As shown in the figure, the columns quantify the number of time steps multiple (i.e., 24 hours) while the rows quantify the number of periods (i.e., 365 days). A single row represents a candidate period (one day). Electricity and heat demand data for certain residential jurisdictions were collected from (Maroufmashat et al., 2015) and increased by a factor of 4 for model verification purposes. For example, the total number of data points of each attribute (parameter) over one year is 8760. Accordingly, a typical day approach application would yield 365 since to each 24 hours corresponds one time step. Raw data of electricity and heat demands are reshaped into a new matrix where the number of rows represents the number of days in one year (365 days) and the number of columns represent the number of hours in one day (24 hours).

$$parameter_{8764} = \begin{pmatrix} parameter_1 \\ parameter_2 \\ \vdots \\ parameter_{8764} \end{pmatrix} \xrightarrow{rearrange} \begin{pmatrix} parameter_{1,1} & \cdots & parameter_{1,24} \\ \vdots & \ddots & \vdots \\ parameter_{366,1} & \cdots & parameter_{366,24} \end{pmatrix}$$

Figure S3. Process of rearranging the dimension of wind speed and electric demand.

The reshaped electricity demand and heat demand profile are displayed in Figure S4. **Error! Reference source not found.**

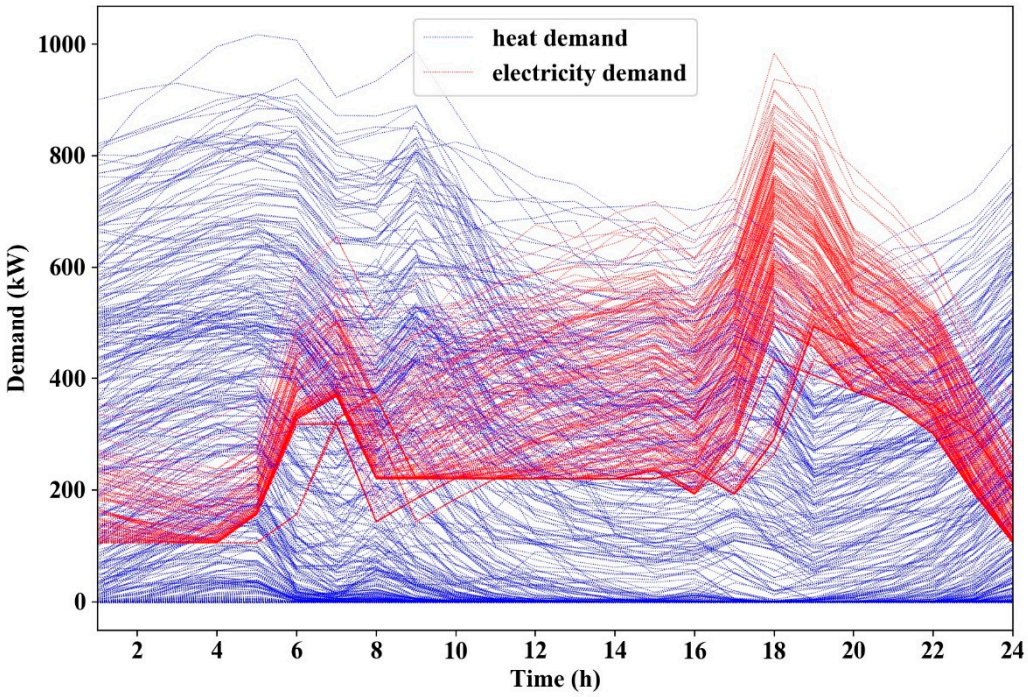

Figure S4. Processed annual electricity (blue lines) and heat demand (red lines) data

The weight factor combinations used to construct the Pareto frontier are reported in Table S1.

Table S1. Multi-objective function weight factors.

Weight Factor	Electricity	Heat
1	0.2	0.8
2	0.3	0.7
3	0.4	0.6
4	0.5	0.5
5	0.6	0.4
6	0.7	0.3
7	0.8	0.2
8	0.9	0.1

Furthermore, the multi-attribute model outputs were assessed using the heuristic clustering algorithm. An entire year (365 days) demand data was clustered into 4,5 and 6 clusters using normal and sequence approaches. The weight factor combinations (see Table S1) were considered to generate each cluster run's Pareto frontier. Twenty-five scenarios were generated

per run. The GAMS/CPLEX (GAMS Development Corporation, 2009) solver was used to perform the runs on an Intel(R) Xeon(R) 2.4 GHz (2 processors), 16 GB RAM workstation. The algorithm tolerance was set to 10^{-3}. The solution times are reported in Table S2. It is worth noticing that the solution time for sequence clustering is slightly shorter than normal clustering due to the extra constraint sets. Also, an increase in the number of clusters expands the model size, and consequent solution time. In general, the model is challenging to solve even with a small number of binary variables.

Table S2. Heuristic algorithm solution times.

Average solution time per scenario (min)	Normal clustering			Sequence clustering		
	4	5	6	4	5	6
	7.03	16.3	26.6	5.98	12.45	23

Pareto frontiers for normal and sequence clustering are illustrated in Figure S5. The Pareto frontiers considered all weight factor combinations shown in Table S1 for all runs. As depicted in Figure S5, increasing the number of clusters has a positive effect over the objective function value (IAE) in both normal and sequence clustering.

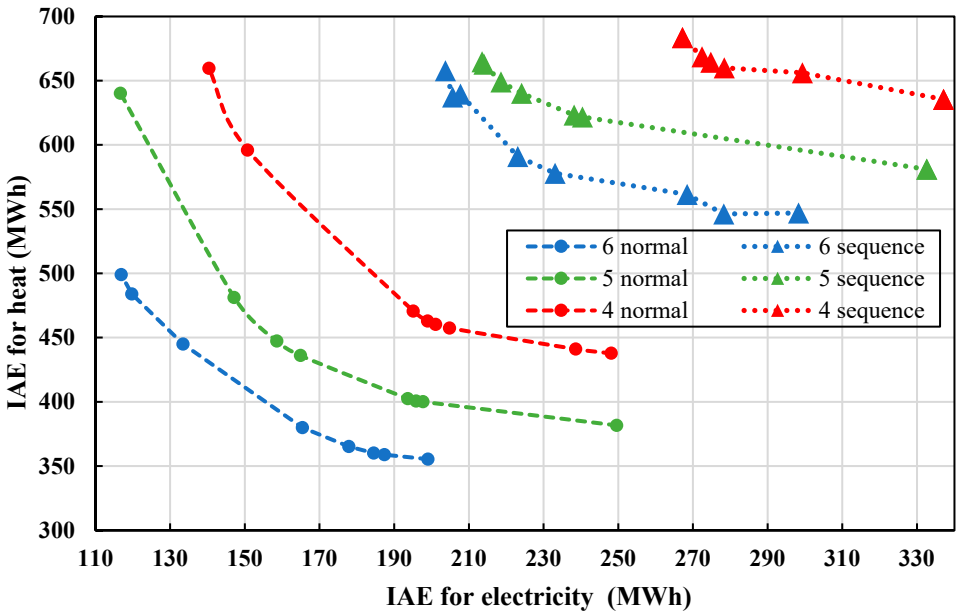

Figure S5. Pareto frontiers for normal and sequence clustering.

A relative error function is employed as validation measure between the cluster and load curves to attain insightful information. This is given as follows:

$$ERROR_{h,d,c} = \frac{D_{h,c} - DL_{d,h}}{DL_{d,h}} \quad \text{(S.1)}$$

where $\mathrm{ERROR_{h,d,c}}$ is the relative error between the cluster and load curves. This metric basically represents the integral absolute error (IAE) or L_1 principle scaled by the cluster curve to evaluate performance independently from the scale of the data set. It also allows comparisons in demand curves significantly differing in magnitude. This error measurement criteria is widely applied in utility forecasting despite the fact that high error values may arise from anomalies instead of simple incorrect predictions (Alhameli,et al., 2019). In order to measure curve similarities within same clusters and dissimilarities between separate clusters, it was calculated the error standard deviation. Average results of relative error for all d days, h hours and weight factors (i.e., 0.5) are presented in Table S3.

Table S3. Computational statistical errors for normal and sequence clustering (365 days-4,5 and 6 clusters)

Clusters		Electricity			Heat		
		Avg	Std	IAE (MWh)	Avg	Std	IAE (MWh)
Normal	4	0.073	0.076	49.3	7.667	36.510	124.500
	5	0.070	0.077	44.5	6.155	2.475	112.125
	6	0.059	0.063	38.75	1.469	7.372	103.285
Sequence	4	0.084	0.094	72.925	11.414	76.977	165.250
	5	0.080	0.087	62.95	6.601	29.838	156.875
	6	0.072	0.084	59.95	5.149	23.637	148.625

Table S3 results show that normal clustering outperforms sequence clustering in terms of objective function value, error average, and standard deviation. This is due to the extra sequence restriction (constraints) that might be a requirement in certain decision-making processes. Furthermore, it is worth noticing that heat demand undergoes significant fluctuations and reaches zero values or close to zero in certain periods (see annual heat demand in Figure S1). Accordingly, relative error calculations were troublesome and amplified. Although the demand ranges from 0 to 1000 kW, the relative error calculation is still difficult. For example, if demand is 10 kW and the cluster value 0.1 kW; the relative error turns into 99%. Moreover, the heat demand's error average and standard deviation are relatively higher than for electricity. This given high fluctuations in heat demand due to seasonal changes such as low heat demand in the summer months (between May and July).

Figure S6 shows the actual heat and electricity demand data and corresponding representative cluster curves using both the normal and sequence clustering approaches (4,5 and 6 normal and sequence clusters). The weight factor used to generate the corresponding representative cluster curves is 0.5 for both heat and electricity attributes. As shown in the figure, clustered data is in good agreement with the actual demand data. However, for heat the clustered curves have a slight discrepancy due to the high fluctuations in the actual heat demand, but generally follows the trend. Also, normal clustering curves match better the actual demand data. Despite the slight error associated with the clustered curves, the purpose of clustering is using a reduced size set of demand data that is well representative and reflects the most probable trends and behavior of the original dataset. These cluster curves reduced-size demand data are used as input for planning, designing, and operating the energy hub model while serving to improve the tractability of the solution.

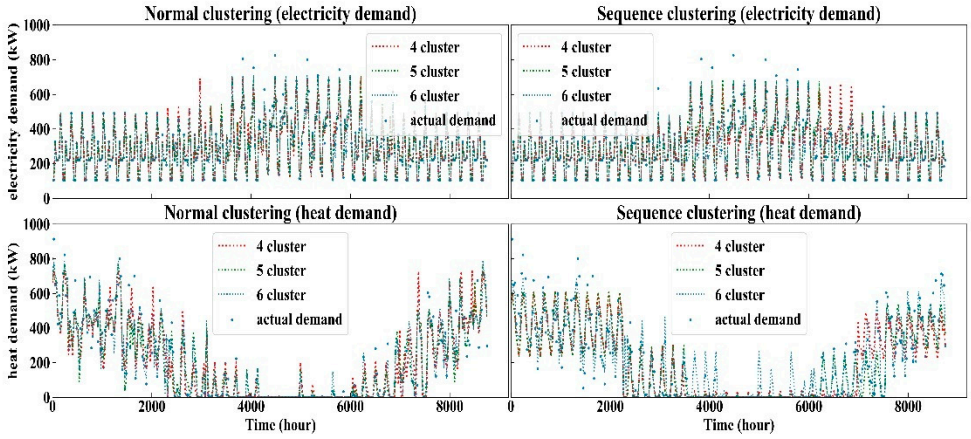

Figure S6. Actual electricity (top) and heat demand (bottom) and their corresponding computed cluster curves (4,5 and 6 clusters) using normal (left) and sequence clustering approaches (right) for 1-year time horizon.

Figures S7 to S12 illustrate the clusters and day assignments of normal and sequence clustering for weight factors 1 and 7 (see Table S1) along with 4, 5, and 6 clusters. Weight factor 1 and 7 prioritize heat electricity demand, respectively. The figures clearly show that clustered curves are slightly affected by weight factors. The main advantage of using the weight factor approach is that allows clustering while emphasizing on one/or more attributes. Normal clustering offers more advantages in terms of flexibility. Also, it was noticed that many electricity demands clusters (especially sequence clusters) overlap with each other. They correspond to different days while their heat demand clusters diverge. Hence, they cannot be merged into the same clusters. In synthesis, the use of normal clustering is recommended to minimize computational effort and deal with large scale models when the applications do not require sequencing.

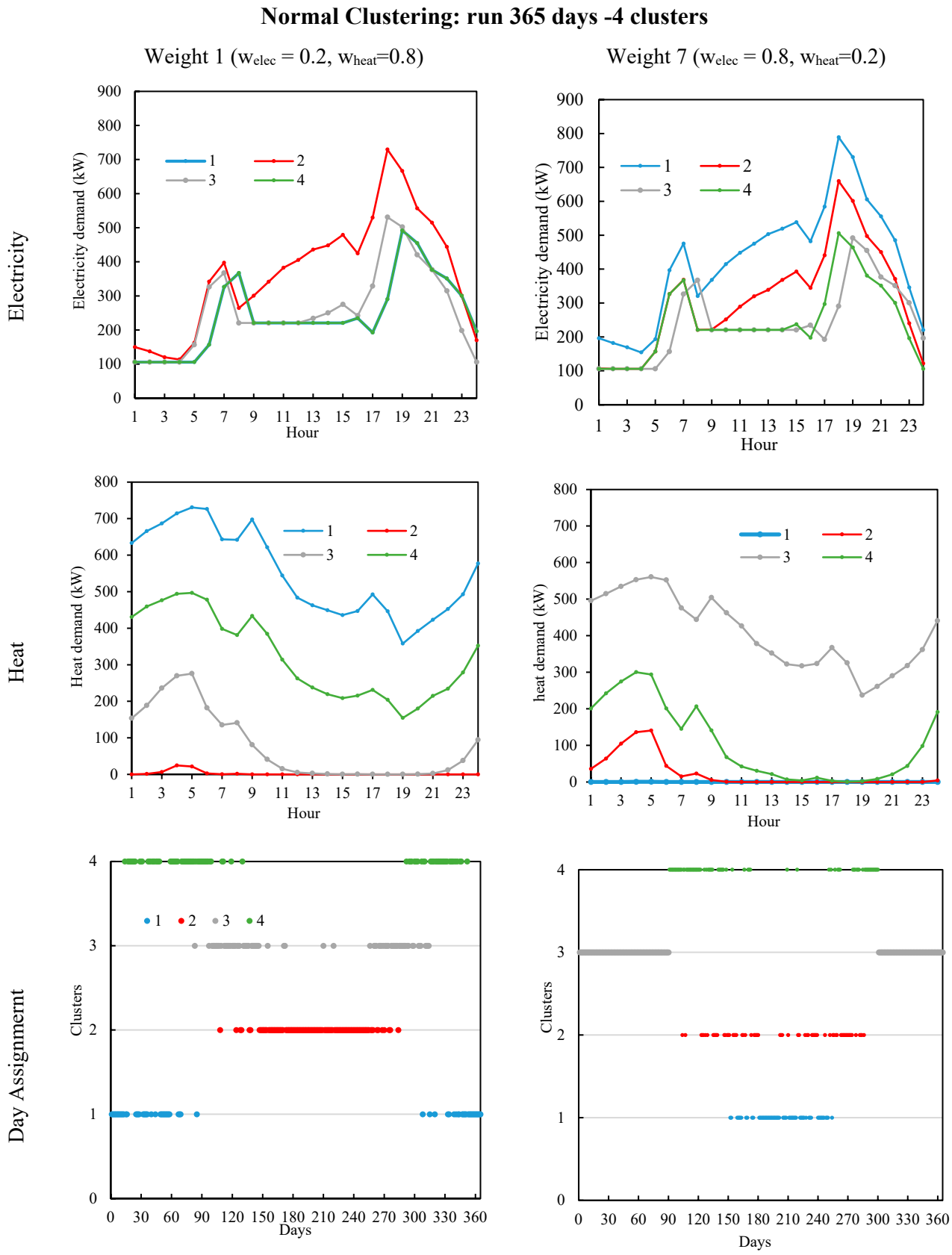

Figure S7. Heat and electricity demand cluster curves with day assignment for weight factors 1 and 8 using 4 normal clustering.

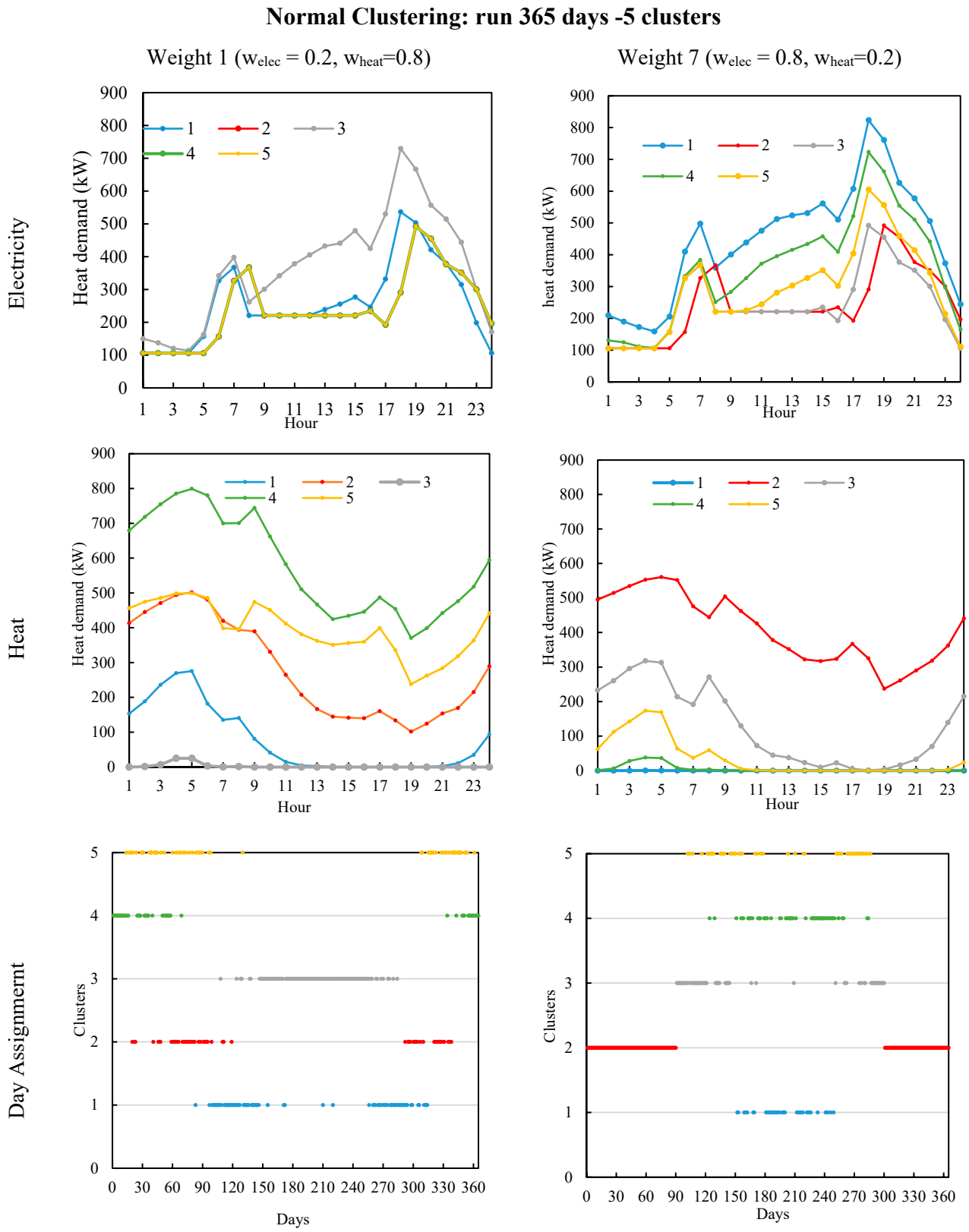

Figure S8. Heat and electricity demand cluster curves with day assignment for weight factors 1 and 8 using 5 normal clustering.

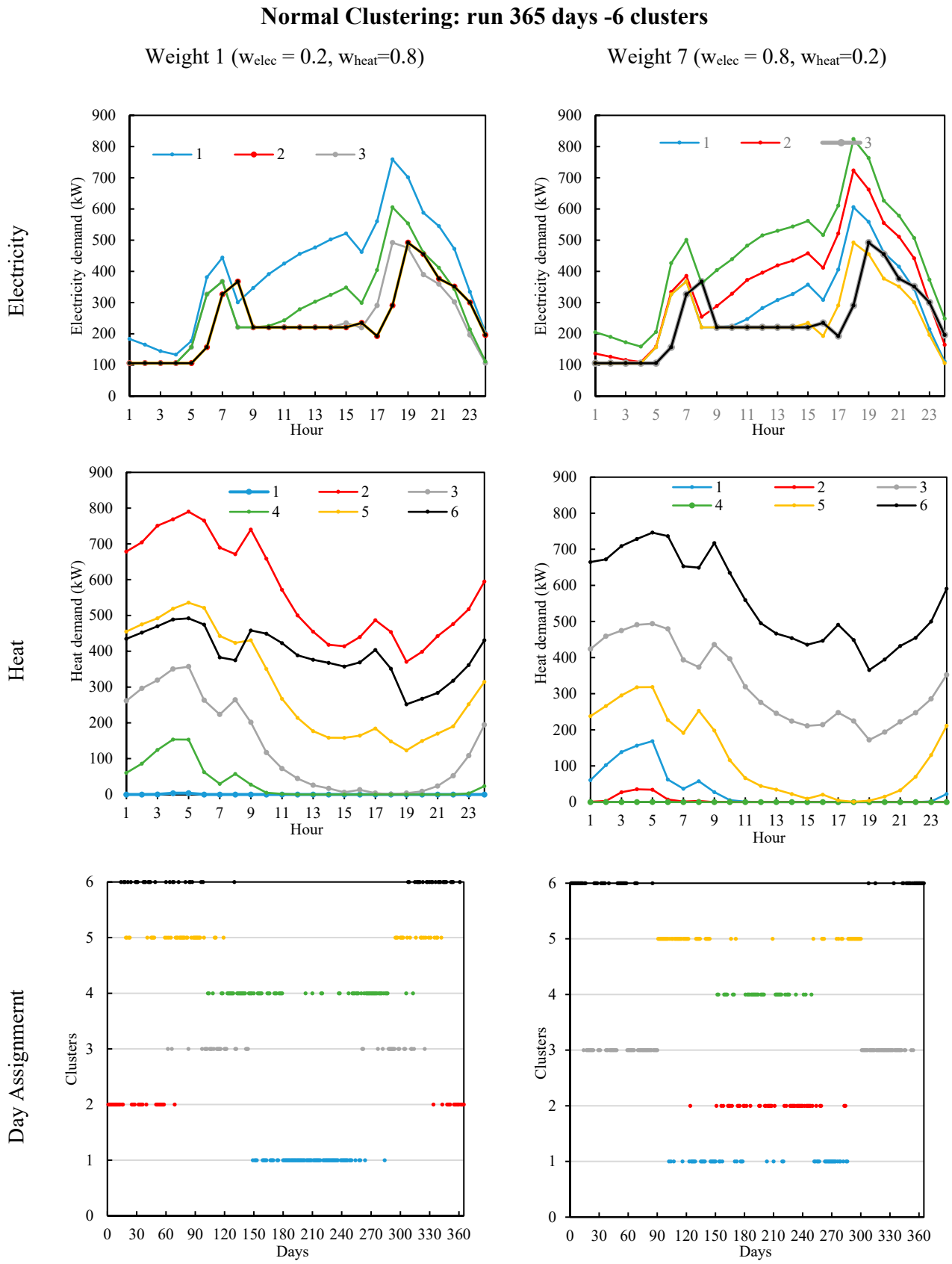

Figure S9. Heat and electricity demand cluster curves with day assignment for weight factors 1 and 8 using 6 normal clustering.

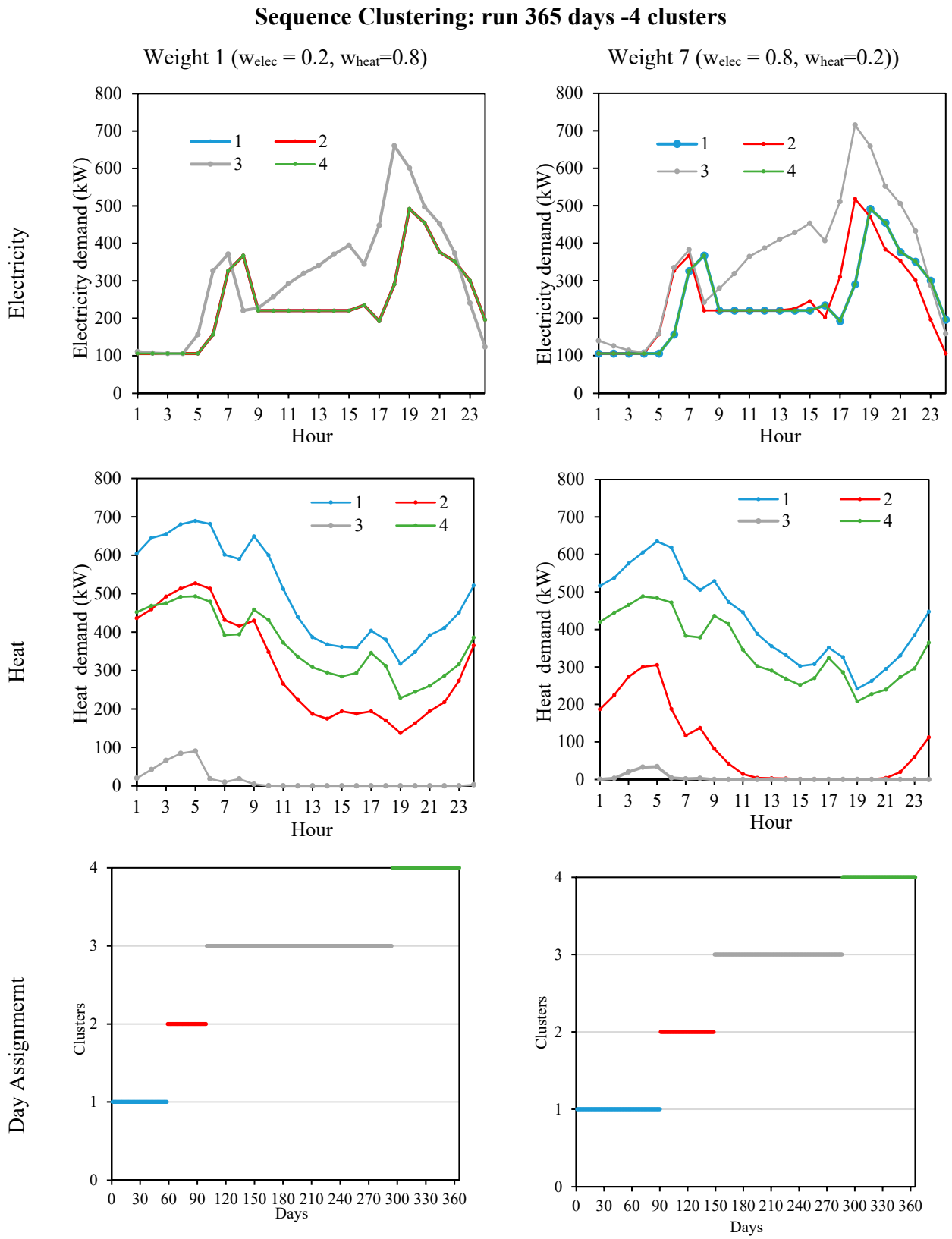

Figure S10. Heat and electricity demand cluster curves with day assignment for weight factors 1 and 8 using 4 sequence clustering.

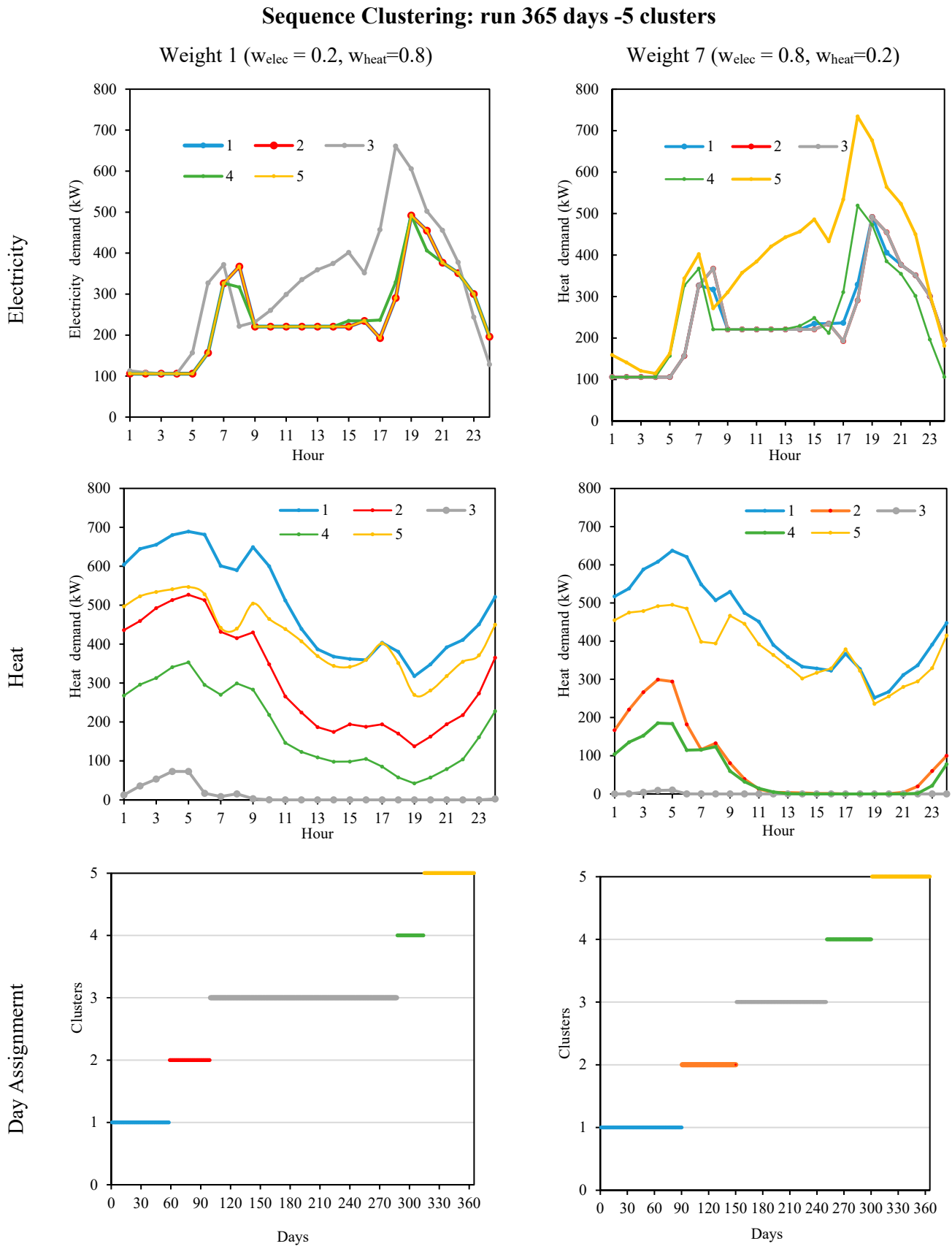

Figure S11. Heat and electricity demand cluster curves with day assignment for weight factors 1 and 8 using 5 sequence clustering.

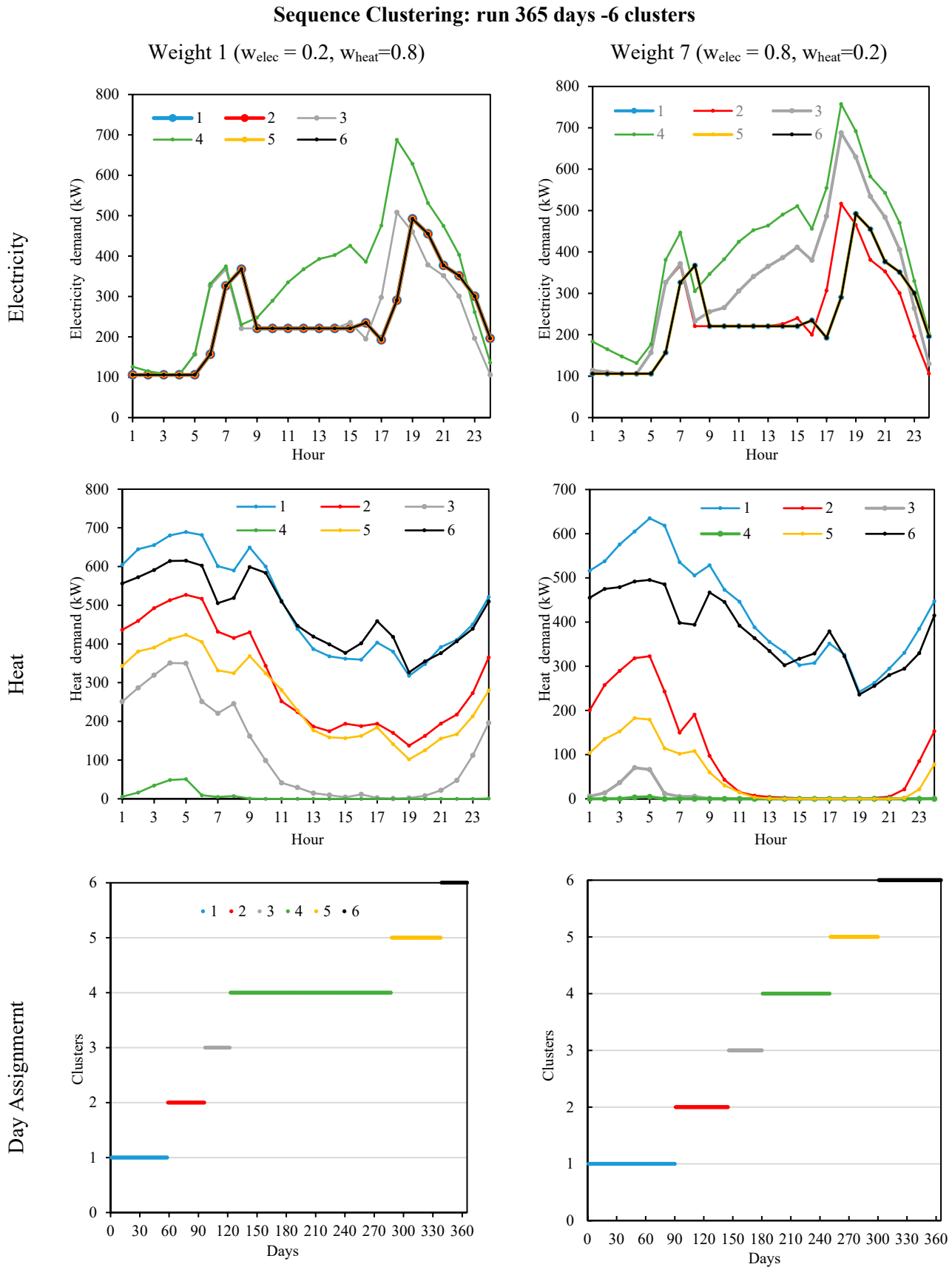

Figure S12. Heat and electricity demand cluster curves with day assignment for weight factors 1 and 8 using 6 sequence clustering.

2. Energy hub model formulation

This subsection discusses the stochastic modeling for the design and operation equations of energy hub system under uncertain wind speeds utilizing clustered demand data (heat and electricity).

The objective function in Eq (S.2) represents the total annual cost including capital cost of the energy hub units and their operating including fuel (gas) consumption, operation, and maintenance costs. The first part of the equation represents the capital cost of the energy hub units (i.e., first stage decision of the stochastic programming). The second part of the equation denotes the annual net cost from operating the energy hub (i.e., basically operational and maintenance and fuel consumption), which depends on the scenario of wind speed uncertainty realization s with probability β_s.

$$min \;\; CRF\left[\sum_{u} y_u \, CAP_u \, E^u_{max} + \sum_{wt} y_{wt} \, CAP_{wt} \sum_{st} y_{st} \, CAP_{st}\right] + \sum_{s} \beta_s \left[\sum_{h,d}\left(\sum_{u}\left[P^u_{i,d,h,s} \, OM_u + NG^u_{d,h,s} Price_{ng}\right] + \sum_{st} P^{st}_{i,d,h,s} \, OM_{st}\right)\right] \quad \text{(S. 2)}$$

where u, st and wt are set of fossils fuel-based power and heat generation units, storing units and wind turbines units respectively. y denotes the integer design variable that represent th number of each unit needed to be installed, $P_{i,d,h,s}$ is the operational decision variable that represent the amount of energy flow (i denote the type of energy heat or electricity) consumed or produced by each energy hub unit at s^{th} scenario and h^{th} hour of the d$^{\text{th}}$ day. CAP and OM represent capital and operational and maintenance cost parameters respectively and $Price_{ng}$ symbolizes the Natural gas price (0.325 \$/m^3) (Maroufmashat et al., 2015).

The capital cost of each unit of the energy hub is obtained by summing the number of installed unit y multiplied by their unit capital cost CAP (\$/unit) (in the case of power and heat generation units (e.g. CHP and boilers) the capital cost is defined as (\$/kW $_{\text{installed}}$), so it is additionally

multiplied by its rated capacities E^{u}_{max}) and converting the present value of the capital cost to annuity ($/yr) by means of the capital recovery factor (CRF). Where $CRF = \frac{r(r+1)^{life}}{(r+1)^{life}+1}$, r (8%) and $life$ (25 years) denote the interest rate and the lifetime of the energy hub respectively. The electricity and heat demands are satisfied at any s^{th} scenario and h^{th} hour of day d through the following energy balances equations as follows Eq. (S.3)-(S.4). Electricity output is fixed to meet demand while heat output is allowed to exceed demand if necessary due to excess heat from CHP units.

$$\sum_{u} P^{u}_{elec,d,h,s} + \sum_{wt} n_{wt} P^{wt}_{elec,s} - P^{elyzr}_{elec,d,h,s} + P^{fuelcell}_{elec,d,h,s} = L_{elec,d,h} \quad , \qquad \forall\, h,d,s \qquad \text{(S.3)}$$

$$\sum_{u} P^{u}_{heat,d,h,s} \geq L_{heat,d,h} \quad , \qquad \forall\, h,d,s \qquad \text{(S.4)}$$

where $L_{elec,d,h}$ (kW) and $L_{heat,d,h}$ (kW) are the hourly electricity and heat demands, respectively. The optimization problem is further constrained by various physical requirements. Each energy hub unit takes in a certain type of energy or mass flow and outputs a different kind of energy or mass flow. A thermodynamic efficiency is used in the following set of equations (Eq. (S.5)-(S.7)) to calculate the amount of utilities produced by energy hub units such as storing units (electrolyzer and fuel cell) power units (CHP) and heat generation units (i.e., boilers). The efficiency of the system depends on the condition and operating regime of the unit, however, for simplicity efficiencies are assumed to be constant for all operating conditions in this study.

$$P^{u}_{i,d,h,s} = NG^{u}_{d,h,s} \eta^{u}_{i} b \quad \forall\, h,d,s,u = \{CHP1, CHP2, CHP3, boiler1, boiler2, boiler3\}, i = \{elec, heat\} \quad \text{(S.5)}$$

where b is the unit conversion factor for the natural gas flowrate (10.7 kWh/m^3).

$$H^{Elyzr}_{d,h,s} = P^{Elyzr}_{elec,d,h,s} \eta^{Elyzr}_{H_2} \qquad \forall\, h,d\,,s \qquad \text{(S.6)}$$

$$P^{Fuelcell}_{elec,d,h,s} = H^{Tank}_{d,h,s} \eta^{Fuelcell}_{elec} \qquad \forall\, h,d\,,s \qquad \text{(S.7)}$$

where $H_{d,h,s}^{Elyzr}$ and $H_{d,h,s}^{Tank}$ is the mass flow rate of hydrogen gas produced by electrolyzer and leaving the hydrogen tank respectively in (kg/hr) at s^{th} scenario and h[th] hour of the d[th] day. The wind turbine, however, is not modeled using aforementioned equations. The power delivered by wind turbine to the electricity grid can be calculated using the following equation (da Rosa, 2013):

$$\mathbb{p}_s^{wt} = \begin{cases} 0 & , v_s < v_{cut\_in}^{wt} \\ C_p \frac{1}{2} \rho_{air} (v_s)^3 A \eta_{wt} & , v_{rated}^{wt} > v_s \geq v_{cut\_in}^{wt} \\ \mathbb{p}_{s,rated}^{wt} & , v_{cut\_out}^{wt} > v_s \geq v_{rated}^{wt} \\ 0 & , v_s \geq v_{cut\_out}^{wt} \end{cases} \quad \text{(S.8)}$$

where *wt* is a the represents the wind turbines types considered in this case study, two wind turbines type where considered namely Vergent (20 kW) and Fuhrlander (30 kW) , the characteristic of these wind turbines can be found in (Stander, 2008) (see Figure S6 in the Appendix). $\mathbb{p}_s^{\mathrm{wt}}$ is a parameter denotes the electrical power generated by one wind turbine in (kw) of type *wt* at scenario *s*. v_s is the actual wind speed in (m/s) at scenario *s*. The wind speed scenarios as well as its corresponding probabilities from **Section 2.3**. are used to calculate the power produced by single wind turbine $\mathbb{p}_s^{\mathrm{wt}}$. $v_{cut\_in}^{wt}$ is wind turbine specific characteristic represents the cut-in-speed, the minimum wind speed at which the turbine blades overcome friction and begin to rotate. Rated output wind speed (v_{rated}^{wt}), for this speed and above, the wind generator is limited to its maximum design output power Cut-out-speed ($v_{cut\_out}^{wt}$) it is a wind speed where braking system is employed to bring the rotor to a standstill to prevent the wind turbine from damage. η_{wt} is the wind generator efficiency. The rotor swept area and the air density are represented by A^{wt} and ρ_{air} respectively. $\mathbf{C_p}$ describes the fraction of the power in the wind that may be converted by the turbine into mechanical work. The maximum

achievable value of C_p is 16/27. The factor 16/27 is known as the Betz limit or Betz efficiency, The Betz limit applies to any type of wind-driven machine (da Rosa, 2013).

Furthermore, Eq. (S.9)-(S.12) determine the number of units that need to be installed (designed) in order to satisfy demand. Also, they ensure that operation of any energy hub unit at any time are within their corresponding capacities as follows:

For boilers and CHP units:

$$P^{u}_{i,d,h,s} \leq y_u \; E^{u}_{rated} \quad \forall\, h,d,s,u = \{CHP1, CHP2, CHP3, boiler1, boiler2, boiler3\}, i = \{elec, heat\} \qquad \text{(S.9)}$$

For electrolyzer (Elyzr)

$$P^{Elyzr}_{elec,d,h,s} \leq y_{Elyzr} \; z^{Elyzr}_{rated} \qquad \forall\, h,d\,,s \qquad \text{(S.10)}$$

For fuel cell

$$P^{Fuelcell}_{elec,d,h,s} \leq y_{Fuelcell} \; z^{Fuelcell}_{rated} \qquad \forall\, h,d\,,s \qquad \text{(S.11)}$$

For hydrogen tank

$$HL_{h,d} \leq y_{Tank} \; z^{Tank}_{rated} \qquad \forall\, h,d\,,s \qquad \text{(S.12)}$$

where z_{rated} is a parameter represent the rating capacity of each energy hub unit (see Table 3 in the main paper). $HL_{h,d,s}$ is the amount of hydrogen stored in hydrogen tank in (kg) at the hth hour of the dth day. From previous equations all energy hub unit output such as power, heat or hydrogen must be less than or equal to the unit rating capacity. The number of wind turbines needed of each wt (wind turbine type) to be installed can be determine using the following equation. In this equation (Eq. (S.13)), the power that can be harvested by wind turbines at each scenario is limited by upper and lower power of single windmill ($\mathbb{p}^{wt}_s$) multiplied by the total number of number wind turbines (y_{wt}). The upper ($\mathbb{p}^{wt}_s(v^{up}_s)$) and lower ($\mathbb{p}^{wt}_s(v^{lo}_s)$) power

of single wind turbine at each scenario corresponds to the upper and lower limits of wind speed of each scenario.

$$y_{wt}\mathbb{P}_s^{wt}(v_s^{lo}) \leq P_s^{wt} \leq y_{wt}\mathbb{P}_s^{wt}(v_s^{up}) \quad \text{(S.13)}$$

Hydrogen gas flows from the electrolyzer to the hydrogen tank where it is stored, until it is directed to the fuel cell when there is need for power generation. In order to keep track of the amount of hydrogen stored at each time, a discretized dynamic mass on hydrogen entering and leaving the tank was applied as described in the following equations (Eq. (S.14)-(S.15)). This equation was designed such that for a given scenario, if the hydrogen production was high due to an excess in wind energy, the excess hydrogen would be stored for use at different scenarios that have low hydrogen production as a result of low wind power. The hydrogen level is not stochastic (not function of uncertain scenarios) but it accounts for all possible uncertain wind speed realization scenarios.

$$HL_{h,d} = HL_{h-1,d} + \sum_s \beta_s\left(H_{d,h-1,s}^{Elyzr} - H_{d,h,s}^{Tank}\right) \quad ,1 < h < 24, \forall d \quad \text{(S.14)}$$

$$HL_{d,h} = HL_{d-1,h} + \sum_s \beta_s\left(H_{d-1,h,s}^{Elyzr} - H_{d-1,h,s}^{Tank}\right) \quad ,h = 1, d > 1 \quad \text{(S.15)}$$

The second equation is added to link between the first hour of the latter day with last hour of the former day. It can be noticed from this equation that the input and output hydrogen flow rates is weighted and summed by the probability of each stochastic scenario to accounts for all possible scenarios.

Since the energy storage technology cannot be charged and discharged simultaneously binary variables ($ch_{d,h,s}$ charging status, $dis_{d,h,s}$ discharging status) are introduced to track the on-off status for the electrolyzer (i.e., works as charging unit) and fuel cell (i.e., works as discharging unit) at each s^{th} scenario and h^{th} hour of the d^{th} day. In the following equations, the big-M formulation is used to ensure no hydrogen and power flow occur out of the electrolyzer and fuel cell when they are off.

$$H_{d,h,s}^{Elyzr} \leq ch_{d,h,s}\ M \quad , \quad \forall\, h, d\, , s \quad \text{(S.16)}$$

$$P_{elec,d,h,s}^{Fuelcell} \leq dis_{d,h,s}\ M\ , \qquad \forall\, h, d\ , s \qquad \text{(S.17)}$$

where M is a big number, $ch_{d,h,s}$ and $dis_{d,h,s}$ are binary variables that represent the on and off states of electrolyzer and fuel cell units at each at each s^{th} scenario and h^{th} hour of the d^{th} day respectively. In order to prevent the electrolyzer (charging status) and fuel cell (discharging states) from running at the same time, the following constraint is added:

$$ch_{d,h,s} + dis_{d,h,s} \leq 1 \quad \forall\, h, d\ , s \qquad \text{(S.18)}$$

3. Further results and discussions

This section presents further results, discussions, and details of the energy hub with hydrogen storage case study. Two subsections provide further details about two of the scenarios under analysis.

3.1. Baseline Scenario

The effect of multi-scale clustering approach of the demand data on the energy hub operational decision are depicted in Figure S13. Accordingly, the figure presents the energy hub total utility production rates for the normal and sequence clustering cases for weight factors 1, 4, and 8. The figures display the error associated with the total utility production using clustered cases relative to the original case. The figure shows that the errors in the total production rate from boilers are higher than the errors associated with electricity and heat production from CHP. This due to the Eq. (S.4) that allows the heat production to be greater than the demand whereas Electricity output is fixed to meet demand. On the other hand, electricity production rates using clustered model is very close to the original model. It can be concluded that using the clustering approach is an effective tool to reduce the size of the original model while maintaining good results. We can say that the proposed clustering multi-scale method is a trade-off between computational effort and data accuracy. Similarly, one can notice that increasing the number of clusters improves the solution quality as it closes the gap between the original (i.e., non-

clustered cases) and clustered cases. In addition, the results of weight factor 1 are much closer to the optimal non-clustered case because it leans towards the heat demand. As the heat demand shows the higher variability among utilities, prioritizing the heat demand allows keeping it closer to the original value. Moreover, as one could expect normal clustering showcases better solution quality than sequence clustering due to the additional restriction added by sequence clustering. The clustered cases energy hub model underestimated the installed design capacities of reboilers since they are cheaper (have less effect on the objective function; thus, the total heat rate generated by reboilers using the clustered case energy hub model are less than the original model).

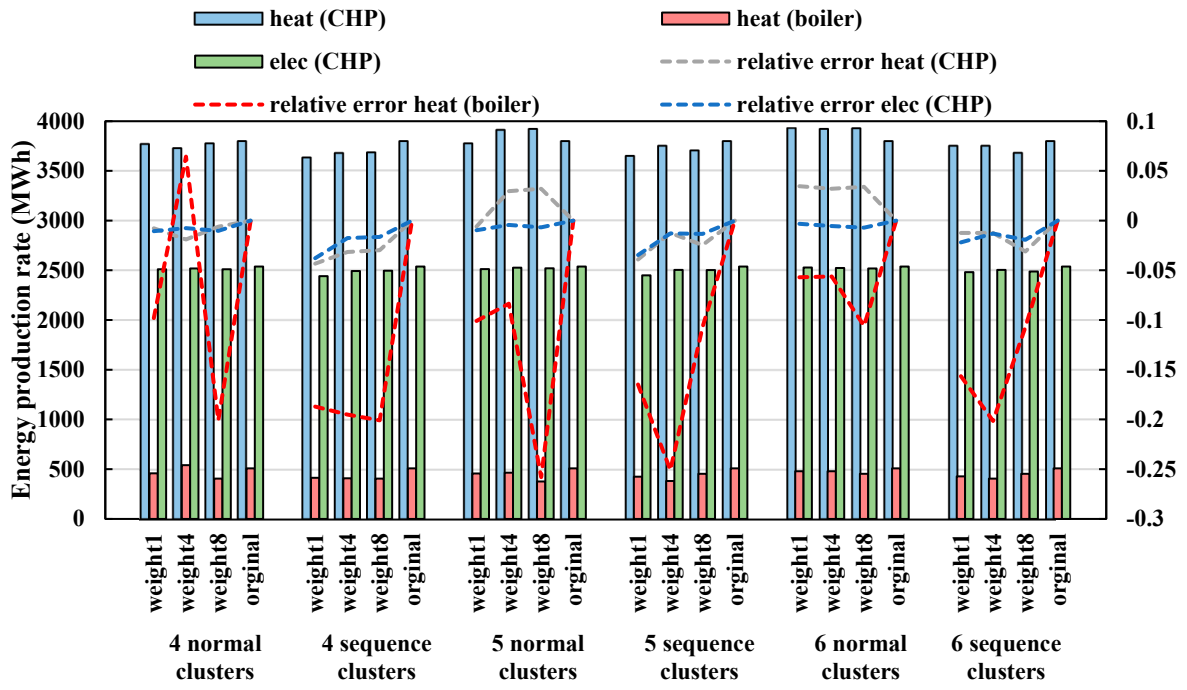

Figure S13. Energy hub's utility production rates comparison between original and clustered model.

3.2. GHG Emissions Constrained Scenario (Further Details)

The higher number of clusters the closer the design decision variable values between the clustered and original model. For example, 5-normal clustering features the same number of CHP100 units as the original case, whereas 6-normal clustering with weight factor 1 shows the

exact same design of the original case. This can be clearly observed in Figure S14 which shows the installed power and heat generation capacity of all clustered runs with weight factor 1,4, and 8 along with the original model results. Moreover, the heat and electricity production rates from all analyzed clustered scenarios are very close to the original model while their relative error do not exceed 20% (see Figure S15 for details).

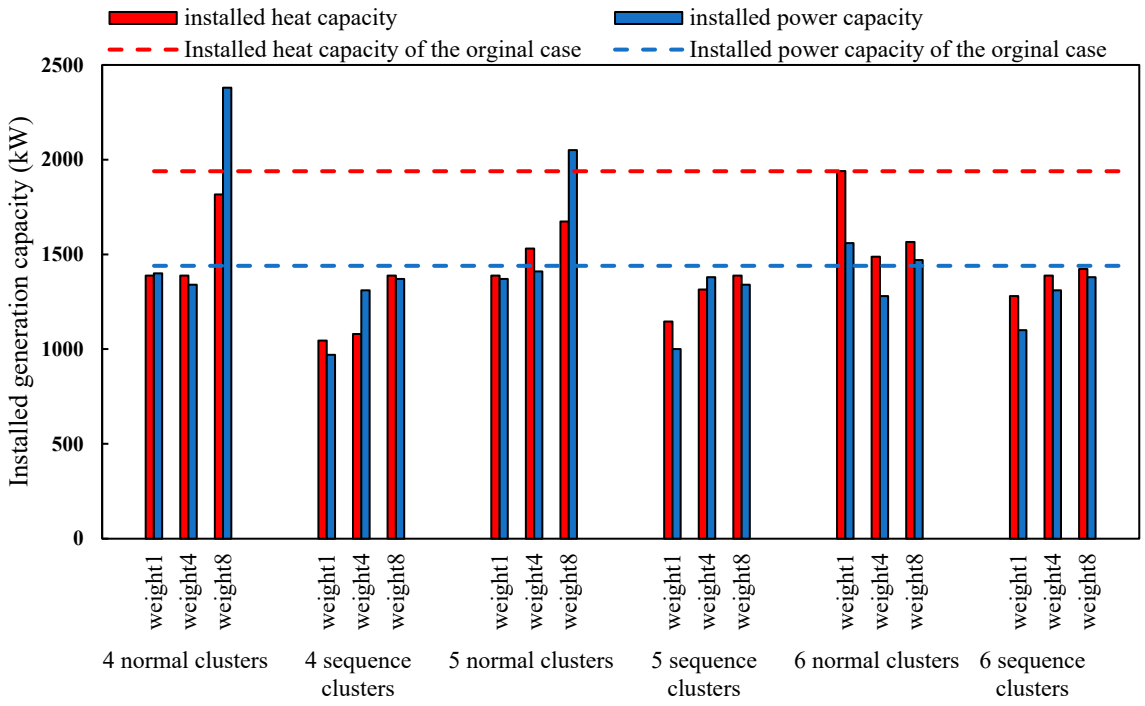

Figure S14. Installed heat and power generation capacity for the energy hub system under the GHG emissions constraint.

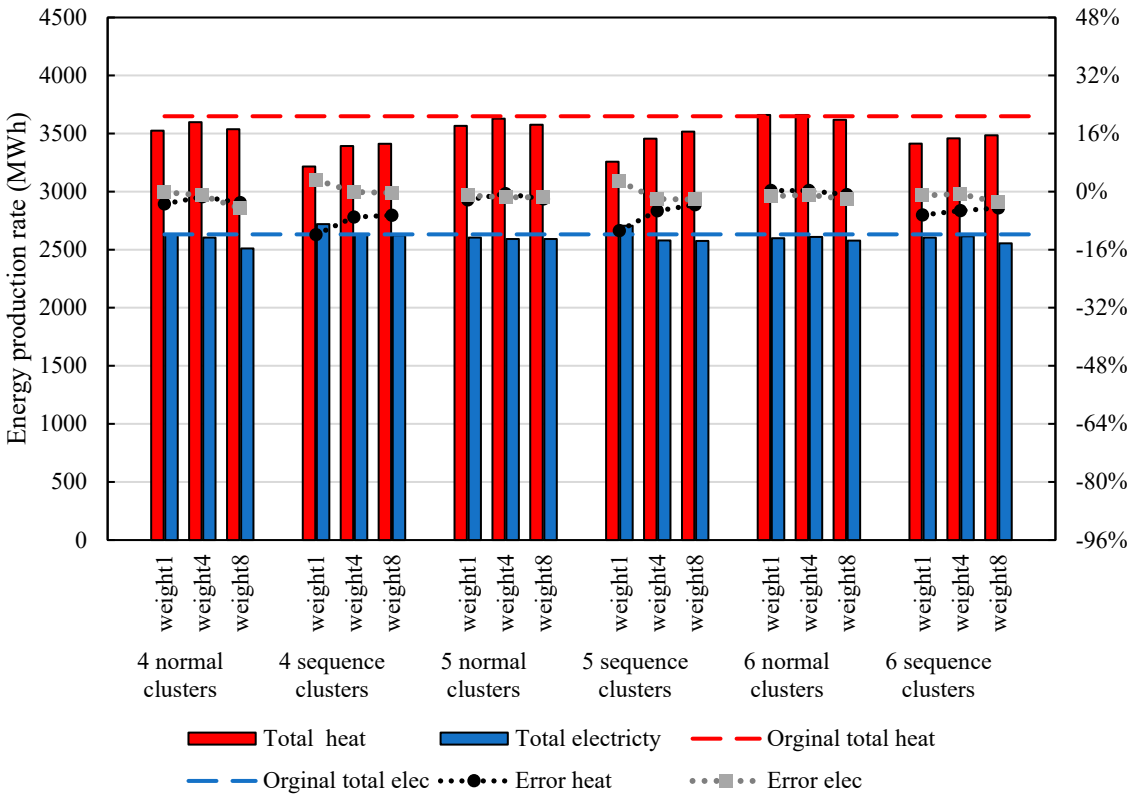

Figure S15. Energy hub's utility production rates comparison between the original and clustered model.

Reference

Alhameli, F.; Elkamel, A.; Betancourt-Torcat, A.; Almansoori, A. A mixed-integer programming approach for clustering demand data for multiscale mathematical programming applications. AIChE J. 2019, 65, e16578. https://doi.org/10.1002/aic.16578

Battelle Memorial Institute, 2017. Manufacturing Cost Analysis: 100kW and 250 kW Fuel Cell Systems for Primary Power and Combined Heat and Power Applications. U.S. Dep. Energy, Fuel Cell Technol. Off. 98, 293.

da Rosa, A., 2013. Wind Energy, in: Fundamentals of Renewable Energy

Processes. Elsevier, pp. 685–763. https://doi.org/10.1016/B978-0-12-397219-4.00015-1

GAMS Development Corporation, 2009. General Algebraic Modeling System (GAMS) Release 23.3.3.

Maroufmashat, A., Elkamel, A., Fowler, M., Sattari, S., Roshandel, R., Hajimiragha, A., Walker, S., Entchev, E., 2015. Modeling and optimization of a network of energy hubs to improve economic and emission considerations. Energy 93, 2546–2558. https://doi.org/10.1016/j.energy.2015.10.079

Maroufmashat, A., Sattari, S., Roshandel, R., Fowler, M., Elkamel, A., 2016. Multi-objective Optimization for Design and Operation of Distributed Energy Systems through the Multi-energy Hub Network Approach. Ind. Eng. Chem. Res. 55, 8950–8966. https://doi.org/10.1021/acs.iecr.6b01264

Stander, J., 2008. The specification of a small commercial wind energy conversion system for the South African Antarctic Research Base SANAE IV.